Talanta 123 (2014) 224–232

Contents lists available at ScienceDirect

Talanta

journal homepage: www.elsevier.com/locate/talanta

Frits coated with nano-structured conducting copolymer for solid-phase extraction of polycyclic aromatic hydrocarbons in water samples and liquid chromatographic analysis

Mina Rahimi [a,b,*], Ebrahim Noroozian [a]

[a] Department of Chemistry, Shahid Bahonar University of Kerman, Faculty of Science, P.O.Box 76169-133, Kerman, Iran
[b] Young Research Society, Shahid Bahonar University of Kerman, Kerman, Iran

ARTICLE INFO

Article history:
Received 26 November 2013
Received in revised form
23 January 2014
Accepted 2 February 2014
Available online 13 February 2014

Keywords:
Nano-structure
Pyrrole
o-Toluidine
Solid-phase extraction
Polycyclic aromatic hydrocarbons

ABSTRACT

A novel nano-structured conducting copolymer of pyrrole and *o*-toluidine was electrosynthesized on steel frit as a new sorbent. The applicability of the frit was assessed for the solid-phase extraction (SPE) of Polycyclic aromatic hydrocarbons (PAHs) by coupling with HPLC–UV. The combination of pyrrole and *o*-toluidine in a copolymer form presents desirable opportunities to produce materials for new applications. The scanning electron microscopy (SEM), energy-dispersive X-ray spectroscopy (EDX) and FTIR spectrum for the coated frit were studied. Improved lifetime and satisfactory extraction efficiency were obtained by doping with dodecylbenzenesulfonate (DBS) and oxalate groups into the framework of copolymer. The effects of potential, time and solution concentration (pyrrole, *o*-toluidine, DBS and oxalic acid) were evaluated in the coating step. The effects of various parameters on the efficiency of the solid-phase extraction process, such as the sample loading rate, elution solvent type, salt effect, volume and flow rate of sample and elution solvent, were investigated. Under optimum conditions, LODs were 0.01–0.08 ng mL^{-1}. The method showed linearity in the range of 0.1–300 ng mL^{-1} with coefficients of determination >0.98. The intra-day ($n=7$) RSDs obtained at an 8 ng mL^{-1} concentration level were $<11.4\%$ under optimized conditions respectively. The recoveries (8 and 40 ng mL^{-1}) ranged from 64% to 119%.

1. Introduction

Threats to agricultural water near the industrial areas are an issue of growing concern, and the need for efficient monitoring of actions is of paramount importance. Polycyclic aromatic hydrocarbons (PAHs) are a group of compounds that are included in the United States Environmental Protection Agency (USEPA) and the European Union (EU) priority pollutant list due to their mutagenic, carcinogenic, and endocrine-disrupting properties [1–4]. The sources of PAHs in the aquatic environment include various routes, such as oil spills, fossil fuels, and domestic and industrial wastewater discharges, as well as atmospheric fallout deposition. Because of the complexity of the PAH matrix and their low concentration in wastewater and surface water samples due to low solubility, the determination of PAHs in such samples is often difficult. Therefore, their separation requires sensitive sample preparation, including efficient extraction, clean up and concentration steps to provide them in a form that is compatible with the analytical instrument [3,5].

Due to advantages of enrichment, high recovery, simplicity, speed, reduction of sample matrix effects, and low organic solvent consumption of solid-phase extraction (SPE) combined with HPLC or GC [6–9] are the most preferred methods for analyzing PAHs in water samples. Adsorption materials, such as metal oxide microspheres [9], amberlite XAD-2 [10], silicabased matrices [11–14], functionalized magnetic nanomaterials [15], multi-walled carbon nanotubes [16,17], coordination polymers [18], metal–organic frameworks [19], gold nanoparticles [20], and zeolites [21], have been recently used for SPE of PAHs. However, some of these materials require multistep preparation or synthetic processes that can be difficult and time-consuming.

In recent years intrinsically conducting polymers such as polypyrrole (PPy) and polyaniline (PANI) and their derivatives have been regarded as the most important conducting polymers, owing to their stability and synthesis advantages [22,23]. The electropolymerization of pyrrole is easy and polypyrrole films generally exhibit better conductivity compared to polyaniline [24,25]. On the other hand, electropolymerization of aniline (and its derivatives) brings about some difficulties like slow nucleation

* Corresponding author at: Department of Chemistry, Shahid Bahonar University of Kerman, Faculty of Science, 22 Bahman Boulevard, Kerman, Iran. Tel./fax: +98 341 3222033.
E-mail address: m_rahimi543@yahoo.com (M. Rahimi).

http://dx.doi.org/10.1016/j.talanta.2014.02.002
0039-9140

and film growth, but its high stability and interesting electrochemical properties have attracted considerable attention [22].

Poly(*o*-toluidine) homopolymer film exhibits good stability but the attempts aiming at the electrosynthesis of poly(*o*-toluidine) film on mild steel surface have failed. In order to obtain a film which combines the advantages of *o*-toluidine (low permeability and high stability) and pyrrole (ease of synthesis and conductivity), poly (pyrrole-*co*-*o*-toluidine) coating has been electrosynthesized [26].

In many reports electropolymerization has been carried out in oxalic acid solution, because acidic environment is suitable for electrodeposition of these polymers and oxalate anion is a counter-ion that not only influences the conductivity of the solution, but also has an important role in polymer surface morphology [27]. PPy films with high conductivity, good stability and good mechanical property can be easily obtained through electrodeposition by using bulky amphiphillic sulfonate dopants, such as dodecylbenzenesulfonate (DBS) [28,29].

Conducting polymers, due to their high electrical conductivity, have been successfully used for SPE and solid-phase microextraction (SPME) [30,31]. Conducting polymers have high extraction efficiency toward aromatic compounds [32]. Their multifunction interactive properties (acid–base interactions, non-polar interactions, dipole–dipole interactions and H-bonding) make conducting polymers unique when used as solid-phase extraction sorbents [33]. Some authors have described the chemical synthesis of polar particles, whose retention properties have been tested in solid-phase extraction of polar compounds, such as PANI [34] and PPy [35].

Nanotechnology applications in SPE coating preparation have shown remarkable growth in recent years [36]. Compared with other materials used for SPE, nanomaterials offer a significant higher surface area-to-volume ratio that promises much greater extraction capacity and efficiency [37]. The nano-structured adsorbents can greatly increase effective surface area, and consequently extraction capacity [38].

This paper reports application of novel nano-structured poly (pyrrole-*co*-*o*-toluidine) as a SPE frit coating. Electropolymerization of the copolymer on a steel frit was carried out in an aqueous mixture of DBS and oxalate anions. A constant potential coulometric (CPC) method was used for the electropolymerization. It was used as a new in-house adsorbent for simultaneous preconcentration of 8 PAHs (as a model): naphthalene (Nap), acenaphthylene (Acy), fluorene (Flu), phenanthrene (Phe), anthracene (Ant), fluoranthene (Flt), pyrene (Pyr) and biphenyle (Bip). These PAHs contain two, three, and four aromatic rings, and the logarithms of their octanol–water partition (log Kow) are from 3.37 to 4.88. The proposed SPE method based on coated frit in conjunction with HPLC–UV was used to determine PAHs in tap water, wastewater and agricultural water samples (Fig. 1). To our knowledge, this is the first report of using nano-structured poly(pyrrole-*co*-*o*-toluidine) adsorbent for the enrichment of organic pollutants from real samples.

2. Experimental

2.1. Reagents and materials

Standard grade PAHs including naphthalene, acenaphthylene, fluorene, phenanthrene, anthracene, fluoranthene, pyrene and biphenyle were purchased from Fluka (Buchs, Switzerland). These compounds were used as-received. Pyrrole ($\geq$97% pure) was obtained from Fluka (Buchs, Switzerland) and was redistilled before use and stored in a dark bottle under nitrogen atmosphere in a refrigerator. *O*-toluidine ($\geq$99.5% pure) was purchased from Merck (Darmstadt, Germany). Sodium dodecylbenzene sulfonate (88% pure) was obtained from Acros (NJ, USA) and oxalic acid was purchased from Fluka (Buchs, Switzerland). Steel frit (20 mm diameter, and 350 μm mesh size) was cut and used as the SPE device after coating with the sorbent material.

A 1000 μg mL^{-1} stock solution of the mixture of PAHs was prepared in acetonitrile. Working solutions were prepared by appropriate dilution of the stock solution in distilled water. Nitrogen ($\geq$99.5%) used for the evaporation of solvents was obtained from local vendors. HPLC-grade acetonitrile (ACN) and methanol were purchased from Merck (Darmstadt, Germany). Other reagents used were of highest purity available. Double distilled water was used in all experiments. All glasswares were obtained from Duran (Elmsford, NY, USA).

2.2. Apparatus

The SPE device was home made. Electrochemical polymerization of copolymer onto the SPE device was carried out by a potentiostat/galvanostat model BHP 2061-C, obtained from Behpajuh (Esfahan, Iran). The Pt counterelectrode and the Ag/AgCl reference electrode used in the electrochemical process were obtained from Azar Electrode (Urumieh, Iran). An ultrasonic bath, Bandelin Sonorex Super (Berlin, Germany), was used for sonication purposes.

The HPLC system from Shimadzu (Tokyo, Japan) consisted of two LC-6A pumps, SPD-6AV UV–vis detector, SCL-6A system controller, C-R6A Chromatopac data processor, Rheodyne 7120 sampling valve with a 20-μL loop and a Zorbax SB-C8 column (5 μm thickness, 4.6 mm × 150 mm). The mobile phase was a mixture of acetonitrile/water (60/40, v/v), with total flow rate of 1.0 mL min^{-1}. Surface morphology was studied by a scanning electron microscope (SEM) using Hitachi S4160 (Tokyo, Japan) and an energy-dispersive X-ray spectroscopy (EDX) model 7431 from Oxford Instruments (Oxford, England). The FTIR spectra of coating were determined by a Mattson 1000 FTIR spectrometer from Unicam (England). A model 7890A, GC coupled with a 5975C quadrupole mass spectrometer and electron impact ion-source from Agilent Technologies (CA, USA) were used for the identification of PAHs in real samples. The MS conditions were mass range 50–400, electron energy 70 eV, GC/MS interface and ion-source temperature of 230 °C.

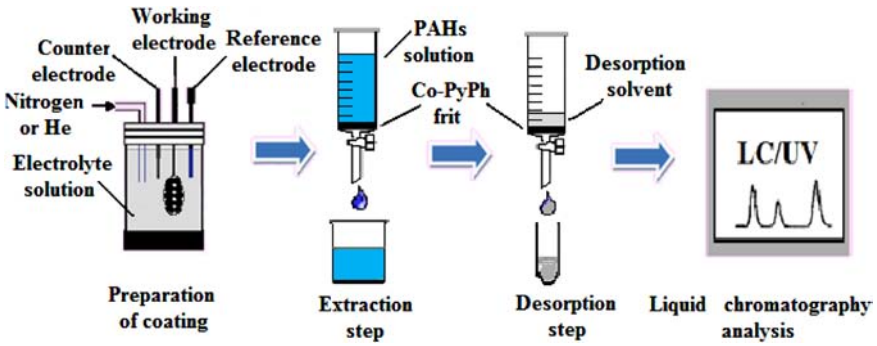

Fig. 1. Schematic diagram of the SPE procedure.

2.3. Preparation of the coating

Electrodeposition of the copolymer of pyrrole and *o*-toluidine was carried out through the CPC method. A solution made up of 0.3 mol L^{-1} pyrrole, 0.02 mol L^{-1} *o*-toluidine, 0.5 mol L^{-1} oxalate and 0.005 mol L^{-1} DBS was used for this purpose. In order to make the SPE device, a piece of steel frit was chosen as the working electrode, a Pt-electrode as the counterelectrode, and an Ag/AgCl electrode as the reference electrode. The coulometric conditions were deposition potential 1.2 V and deposition time 1500 s. To make the coating adhere firmly to the surface of the frit, the surface of the frit was first roughened by a smooth sand paper and then washed in water and then acetone while sonicating for 15 min. After deposition, the coating was washed with distilled water several times. The frit now coated with 160 mg copolymer was used as the sorbent for SPE of polycyclic aromatic hydrocarbons.

2.4. SPE procedure

The efficiency of the coated frit was determined by applying different volumes of PAHs in 20 ng mL^{-1} concentration. In general, the conditioning step is important for the cartridge so as to adapt to the same physicochemical properties of the samples. Therefore, the coated frit was conditioned by successive elution of 5 mL acetonitrile and 5 mL water. Water samples (50 mL) spiked with PAHs at known concentration (20 ng mL^{-1}), to study extraction performance and optimize the extraction conditions, were passed through the column at a flow rate of 1 mL min^{-1} by force of gravity. The frit was cleaned up with 1 mL distilled water and dried with nitrogen gas. Then, the retained analytes were eluted from the frit by 4 mL solvent at a flow rate of 1.0 mL min^{-1}. After desorption, the solvent was evaporated under a gentle stream of nitrogen, the dried residue was redissolved in 100 μL of acetonitrile and then 20 μL of the resulting solution was injected to HPLC for analysis. To reuse the frit in further analysis, it was placed in 4 mL of ACN for 30 min. Blank assays were also performed using the same procedure as described above, employing double distilled water without spiking.

3. Results and discussion

3.1. Characterization of nano-structured copolymer

3.1.1. Properties of coating

The physical properties of the copolymer coating, such as morphology, porosity, mechanical property and thermal stability, are influenced by the counter-ions used [39,40]. This opens the possibility for producing a smooth and adherent copolymer coating by using a simple one-step electropolymerization process and DBS as the counter-ion [26,27,41].

The surface characteristics of coated poly(pyrrole-*co*-*o*-toluidine) were investigated by SEM and EDX techniques. Fig. 2a shows the micrograph of a nano-structured copolymer. For comparison, the SEM micrograph and the EDX spectrum of polypyrrole prepared were studied (Fig. 2b). The morphology of polypyrrole and copolymer films shows a cauliflower-like structure constituting spherical grains in both cases. However, the size of the grains in the cauliflower structure of copolymer is much smaller than the size in PPy indicating a larger surface area (Fig. 2a). The existence of sulfur in the EDX spectrum indicates that the anionic surfactant, DBS, is incorporated into the polymer structure (Fig. 2a and b).

As illustrated in Fig. 2a, the morphology of coating surface contains agglomeration of nano-sized particles below 750 nm. Porous structure of the frit surface is evenly distributed. The nano-structure of the film provides high surface area and then large stationary phase loading and high extraction capacity. The porous surface structure of the copolymer film and dipole–dipole and hydrogen bonding interactions could be major reasons for strong retaining behavior of this sorbent towards an analyte. The sorption mechanism for the analyte into the copolymer frit is adsorption similar to the other solid porous coatings.

FTIR spectra of polypyrrole and copolymer samples are shown in Fig. 3. It was reported that the bands centered at 3580 and 3463 cm^{-1} were related to characteristic –NH-stretching vibration. This indicated the presence of –NH-groups in *o*-toluidine and pyrrole units that were seen in all spectra. FTIR spectrum of polymerized PPy and copolymer showed that the band intensity at 1550 and 1516 cm^{-1} corresponds to the pyrrole ring. In Fig. 3, peaks at 1625 cm^{-1} and 1630 cm^{-1} are related to C–N═C bond in the spectrum of PPy and copolymer respectively. In the FTIR spectrum of polypyrrole, the peak at 1036 cm^{-1} is due to –C–H in-plane deformation of the pyrrole unit. It was reported that in the spectrum of the copolymer sample the peak at 2900 cm^{-1} is due to characteristic aromatic –C–H stretching. Also, the peak at 1290 cm^{-1} is attributed to methyl group in the structure of *o*-toluidine unit. The FTIR spectrum of synthesized copolymer in mixed oxalic acid and DBS showed that the special peaks that belong to S═O stretches were located at 1040 cm^{-1} and accordingly the peak for SO_3 was located at 1191 cm^{-1} (Fig. 3b). The strong band 2900 cm^{-1} can be associated with aliphatic C–H in spectra of copolymer. In the FTIR spectrum of copolymer the single peak at 833 cm^{-1} characterizes a 1,4-substitution and demonstrates that the polymerization occurs via the coupling of the phenyl ring in the para-position [42]. The peaks observed in the FTIR spectrum of poly(pyrrole-*co*-*o*-toluidine) indicated the presence of *o*-toluidine unit in the obtained copolymer structure as shown in Fig. 4.

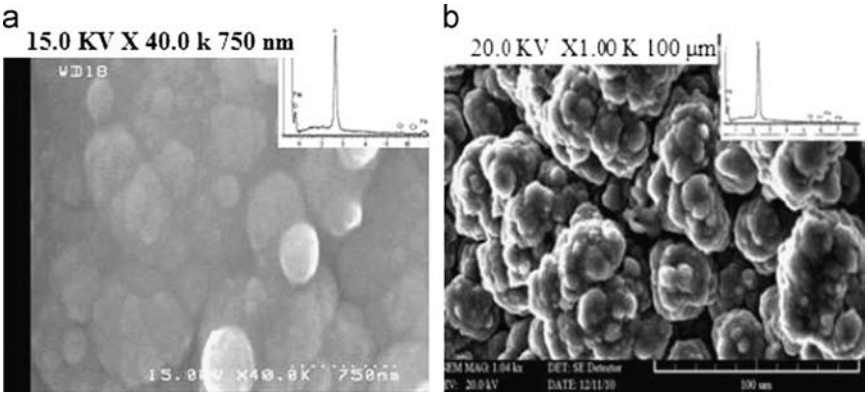

Fig. 2. Scanning electron micrographs and EDX spectra of the surface of PPy and nano-structured poly (pyrrole-*co*-*o*-toluidine). Magnification: (a) 40,000 ×, (b) 1000 ×.

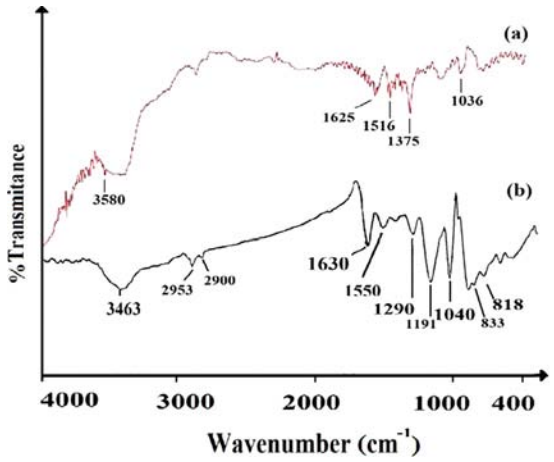

Fig. 3. FTIR spectra of a) PPy and b) nano-structured poly (pyrrole-*co*-*o*-toluidine).

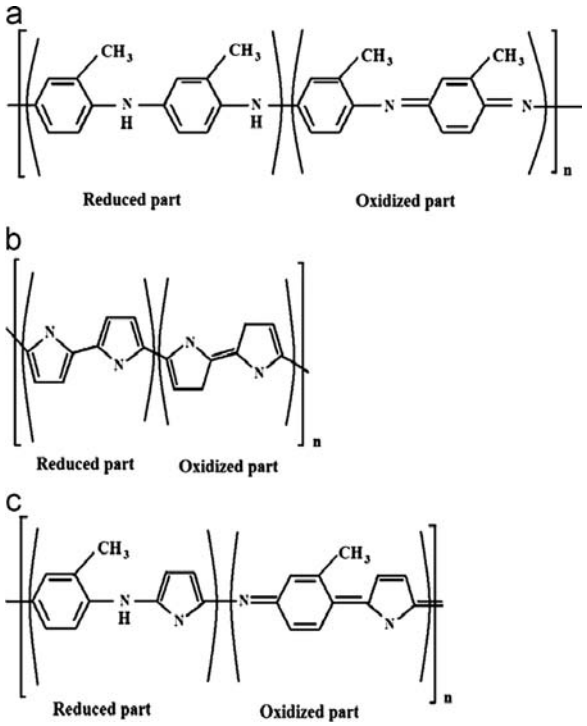

Fig. 4. The structural representation of a) polypyrrole, b) poly *o*-toluidine and (c) poly(pyrrole-*co*-*o*-toluidine).

3.1.2. Repeatability and lifetime of coating

Tolerance of the extraction efficiencies of new copolymer frit in various lifetimes and the repeatability of it were investigated. An acceptable frit-to-frit repeatability (RSD $<10.3\%$, $n=3$) was obtained, indicating that the new frit could be prepared by electrodeposition synthesis in a reproducible manner. Also this sorbent adheres well to the steel frit, so that the prepared frit can be used for SPE analyses many times, without an obvious decrease in extraction efficiencies.

3.2. Coating optimization

A "one-at-a-time" strategy was used to optimize the various parameters affecting the copolymer coating process and SPE experiments.

3.2.1. Electrodeposition by CPC

In order to obtain adherent, smooth, uniform and stable coatings in this process, two parameters including electrode potential and deposition time were optimized. After conditioning the coated frit, it was used for solid-phase extraction of PAHs. The chromatographic peak areas were used to evaluate the extraction efficiency of analytes under various conditions.

3.2.1.1. Effect of potential and deposition time. To optimize the potential, polymerization was initially carried out from a solution containing 0.03 mol L^{-1} DBS, 0.4 mol L^{-1} oxalic acid, 0.01 mol L^{-1} *o*-toluidine and 0.09 mol L^{-1} pyrrole. A 25 mL aliquot of the above solution was placed in an electrochemical cell and polymerization was carried out at various potentials. In these experiments, the deposition time was 1500 s. Since it was not possible to obtain a stable and an adherent poly(*o*-toluidine) film on metal surface (neither platinum nor steel) via electropolymerization, the copolymers of *o* -toluidine and pyrrole were studied. The monomer oxidation potential value of pyrrole was also reported to be around +0.70 V in the literature [26]. Therefore, the oxidation of pyrrole and *o*-toluidine monomers could be achieved simultaneously. Then they formed radical cations that could combine to yield a copolymer structure. With respect to the data shown in Fig. 5a, a potential of 1.2 V was selected for further experiments.

For the evaluation of deposition time, electrochemical deposition was carried out under same conditions as described in the previous paragraph, but at different deposition times (500–3500 s). With respect to the data shown in Fig. 5b, 1500 s was found to be the optimum time. Higher times resulted in thicker coatings with less adhesion. This is in agreement with the results reported by Olszowy et al. [31]. Therefore, 1500 s was selected as deposition time for further experiments.

3.2.1.2. Effect of concentrations. The concentrations of pyrrole, *o*-toluidine, DBS and oxalate were varied on a one-at-a-time basis from 0.05 to 0.4, 0.005 to 0.04, 0.001 to 0.06 and 0.2 to 0.6 mol L^{-1}, respectively. The results obtained are shown in Fig. 6. The highest efficiencies were obtained at 0.3 mol L^{-1} pyrrole, 0.02 mol L^{-1} *o*-toluidine, 0.005 mol L^{-1} DBS and 0.5 mol L^{-1} oxalate. Dodecylbenzene sulfonate is a suitable dopant for preparing a more stable and robust copolymer SPE coating and in addition can be used as a surfactant for preparing nano-structured copolymer. It has been observed that at high DBS concentrations the doping ratio decreases [33]. This is because in high concentration of DBS, the interaction between surfactant molecules gets stronger than that it gets in the lower concentration. Therefore, it is hard for the DBS to incorporate into the copolymer chain as a dopant. Small anions are less able to act as counter-ions in the polymer matrix when DBS is also present [33]. This may be the reason why oxalate concentrations higher than 0.4 mol L^{-1} reduce the extraction efficiency. Also, the high concentration of DBS and oxalate decrease the adhesion of coatings and coated frit lifetime is reduced. For these reasons, a 0.1 mol L^{-1} DBS and a 0.4 mol L^{-1} oxalate were selected for further studies.

3.3. SPE optimization

In order to ensure good selectivity and sensitivity, the frits were conditioned on a daily basis by treating them with acetonitrile for 20 min, rinsed with distilled water and dried using a lint-free tissue. In order to optimize the extraction conditions, the effects of several parameters, including sample loading and elution rate, type and volume of solvent, were studied.

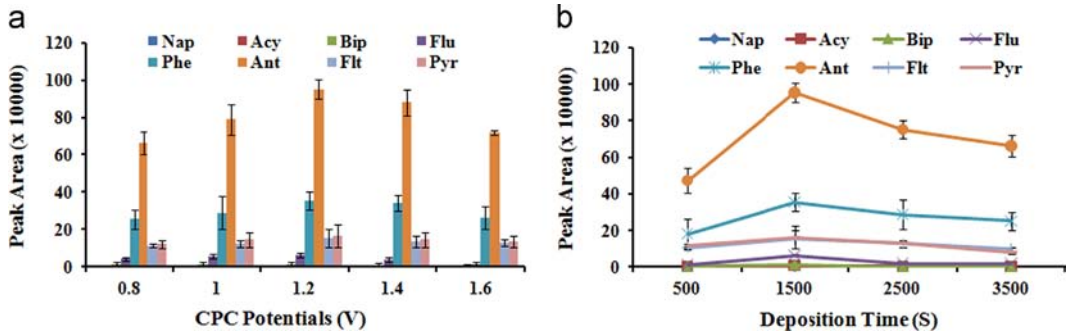

Fig. 5. Effect of coating parameters on the extraction efficiency: a) deposition potential and b) deposition time; $n=3$.

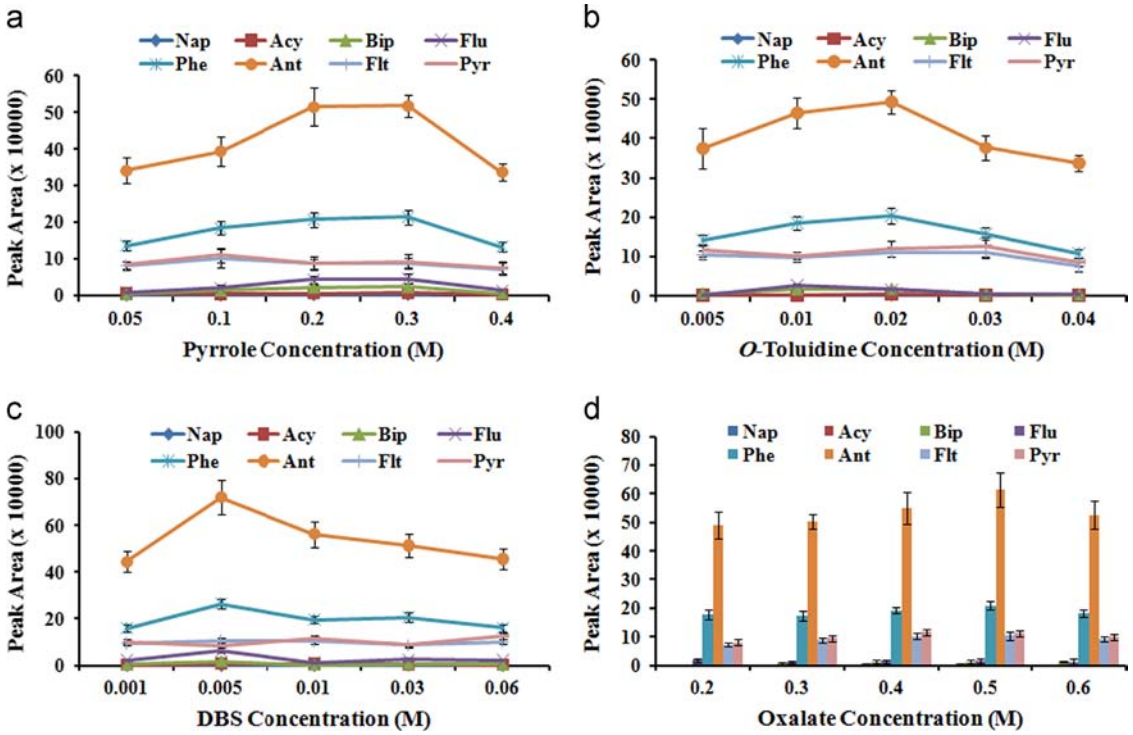

Fig. 6. Effect of coating parameters on the extraction efficiency: concentrations of a) pyrrole, b) *o*-toluidinem c) DBS and d) oxalic acid; $n=3$.

3.3.1. Selection of elution solvent and effect of salt concentration

In the elution step, the adsorbed analytes are removed from the solid sorbent and are transferred to a liquid phase that is suitable for analytical measurement. The desorption of the analytes from the sorbent takes place by the addition of an organic solvent capable of breaking interactions between the active sites of the sorbent and the trapped analytes. For this purpose, acetonitrile, dichloromethane, methanol and n-hexane were selected. 50 mL of aqueous solution 20 ng mL^{-1} of each PAH was passed through the copolymer frit at 1 mL min^{-1} loading rate. Frit clean-up and drying were carried out by 1 mL distilled water and nitrogen gas, respectively. Elution of analytes was performed by 4 mL of various solvents at 1 mL min^{-1}. The results obtained are shown the Fig. 7a. Here, it is seen that dichloromethane is the most suitable solvent for elution of studied PAHs and was selected as a proper elution solvent.

The mechanism of mass transfer of analytes in SPE can be influenced by ionic strength. In addition, the solubility of the non-polar organic solutes in water decreases in the presence of salts. Thus, it is expected that the addition of salts should modify the adsorption of analytes by SPE coating. Therefore, in the present work, the ionic strength of the samples was adjusted by the addition of NaCl from 0% to 8% (w/v). It was observed that the extraction efficiency of PAHs increased with NaCl concentrations up to 2%, and then decreased (Fig. 7b). It seems that the salting out effect played a key role in the extraction procedure up to this point. Here, the water molecules form hydration spheres around the ionic salt molecules, which reduce the concentration of water available to dissolve the analytes. Thus, it is expected that this would drive an additional analyte into the extraction phase [43]. The extraction efficiency decreased at a salt concentration higher than 2% (w/v). This may be explained by the fact that the addition of salt would change the viscosity of the solution and the physical properties of the Nernst diffusion layer in such a way that the diffusion rate of the target analytes into the SPE coating reduces and consequently prolongs the extraction time [44]. Another explanation is that salt deposition onto the coating material decreases the coating porosity [44]. Based on these results, 2% (w/v) NaCl was added to all samples in further experiments.

3.3.2. Effect of elution volume and elution rate

Various volumes of dichloromethane were tested for the elution of PAHs from the solid sorbent, ranging from 4 to 10 mL

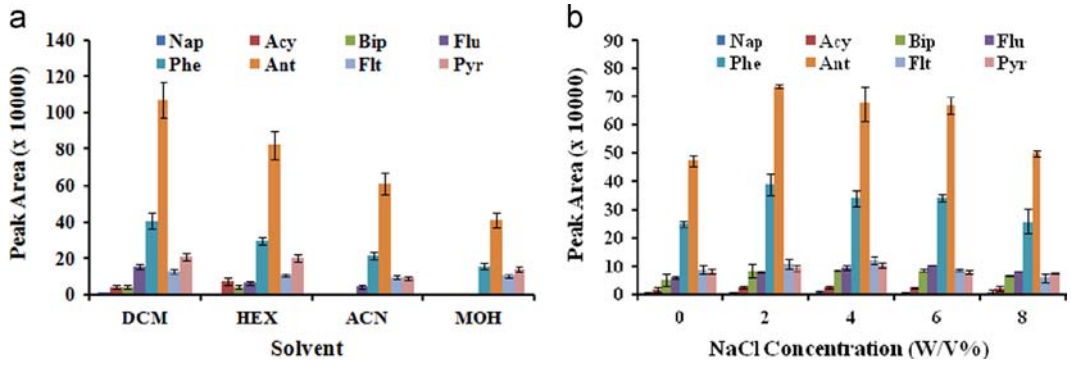

Fig. 7. Effect of a) type of elution solvent and b) NaCl concentration on extraction efficiency; $n=3$.

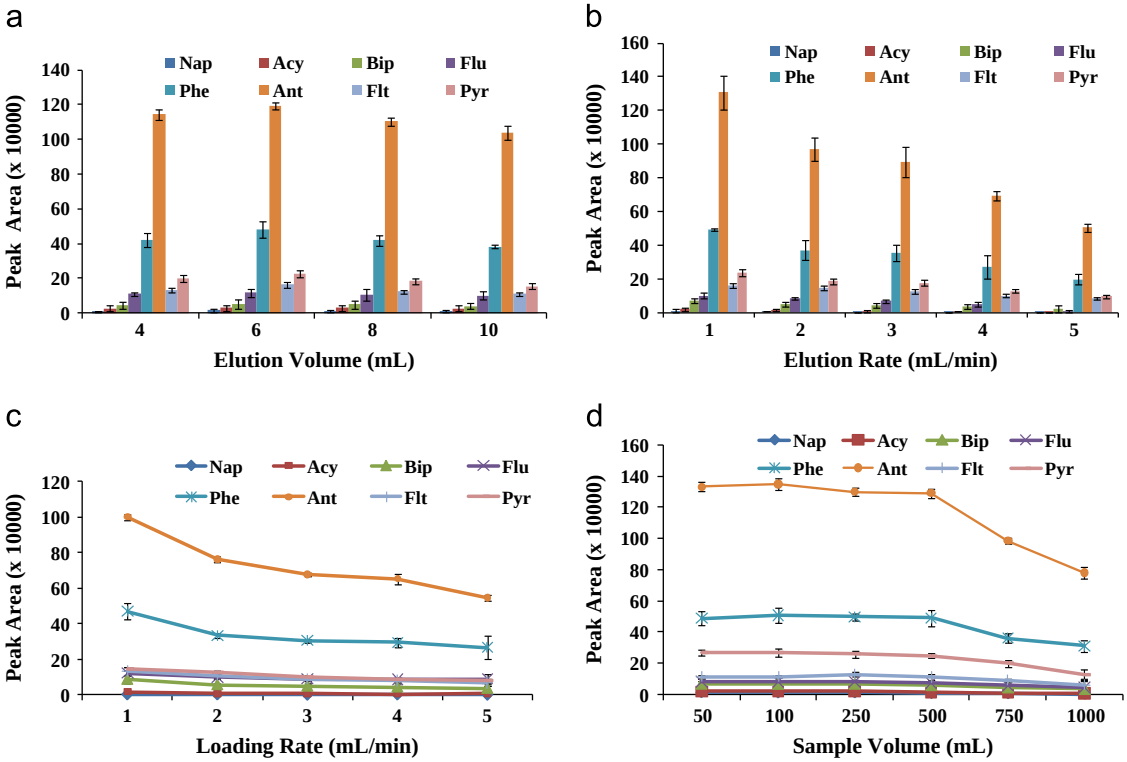

Fig. 8. Effect of a) elution solvent volume, b) elution rate, c) loading rate and d) sample volume on extraction efficiency; $n=3$.

of the solvent. The results obtained are presented in Fig. 8a. Maximum peak area was obtained with 6 mL of the solvent, and therefore this volume was chosen for the elution of the PAHs.

The extraction efficiencies of the compounds are also governed by the flow rate of the eluting solvent through the copolymer frit. Generally, high flow rates result in poor recoveries, while low flow rates result in high recoveries. Five elution rates of 1, 2, 3, 4, and 5 mL min^{-1} were tried for the extraction of PAHs. The results of these experiments are shown in Fig. 8b. Based on these results, an elution rate of 1 mL min^{-1} was selected as the optimum value.

3.3.3. *Effect of loading rate of sample and sample volume*

Loading of the sample takes place immediately after conditioning the cartridge. The introduction of sample takes place under vacuum at a flow rate that permits the adsorption of the target PAHs to the stationary phase. Then, it is important to control the flow rate in this step to promote efficient mass transfer of the analytes to the sorbent. At higher flow-rate, a non-equilibrium process can lead to lower retention volumes of the analytes [45]. Therefore, a suitable flow rate must be selected to achieve high extraction efficiency and reduce loading times. In the present work, samples are percolated through the sorbent bed, simply by gravity. For this purpose, the sample was loaded on the frit at various flow rates. Flow rates were varied between 1 and 5 mL min^{-1} by adjustment of the valve. Differing peak areas were attributed to different extraction efficiencies at various loading rates. The peak areas of most PAHs slightly decreased with the increase of the sample loading flow-rates. Fig. 8c shows the results obtained. Based on these results, a flow rate of 1 mL min^{-1} was selected for the optimum value. At flow rates greater than1 mL min^{-1}, a decrease in the extraction efficiency was observed in the case of all the PAHs.

One important parameter to be controlled in developing an SPE method is the breakthrough volume, i.e. the sample volume where the analyte starts to be eluted from the column end. This parameter depends on the packing efficiency of the sorbent bed and on the strength with which the analytes are retained by the sorbent [46]. Breakthrough volume restricts the maximum sample volume which can be used and hence the maximum preconcentration factor that can be achieved.

Table 1
Limit of detection (LOD), linear range (LR), coefficient of determination (r^2), precision (RSD%) and real samples of the present method.

Compound	LOD[a](ng mL^{-1})	LR (ng mL^{-1})	r^2	RSD%		Concentration found (ng mL^{-1})	
				Intra-day (n=7) 8 (ng mL^{-1})	Frit-to-Frit(n=3) 8 (ng mL^{-1})	Wastewater	Agricultural water
Nap	0.08	0.5–300	0.9925	11.4	10.3	ND[b]	ND
Acy	0.04	0.1–300	0.9898	6.1	5.3	ND	ND
Bip	0.06	0.1–300	0.9886	3.2	9.1	ND	ND
Flu	0.02	0.1–300	0.9933	7.1	7.7	7.9 ($\pm$0.04)[c]	ND
Phe	0.03	0.1–300	0.9915	3.7	3.9	5.8 ($\pm$0.06)	2 ($\pm$0.03)
Ant	0.01	0.1–300	0.9811	4.1	6.9	6.9 ($\pm$0.07)	ND
Flt	0.03	0.1–300	0.9973	3.5	2.4	ND	5.2 ($\pm$0.08)
Pyr	0.02	0.1–300	0.9969	3.2	6.8	6.1($\pm$0.09)	4.8 ($\pm$0.05)

[a] Based on S/N=3.
[b] ND means not detected.
[c] Each figure indicates SD.

Table 2
Comparison of the proposed method with some other methods for extraction and determination of polycyclic aromatic hydrocarbons.

Method	Detection	LOD (ng mL^{-1})	Linear range (ng mL^{-1})	RSDs (%)	Recoveries (%)	Water type	Refs.
LPME[a]	GC–FID[b]	0.07–1.67	0.25–300	1.1–12.6	27–78	Well, tap, sea water	[47]
LDS-SD-DLLME[c]	GC–MS[d]	0.004–0.039	0.05–50	$\leq$11	67–94	Rain water	[48]
HS-SPME[e]	GC–IDMS[f]	–	0.005–9	$\leq$20	79–110	Urine sample	[49]
CFME[g]	GC–MS	0.001–0.01	0.05–15	7–25	70–125	Tap water	[50]
CPE[h]	HPLC–FL[i]	0.023–0.23	0.3–80	2–8	72–99	Sea water	[51]
MA-HS-SPME[j]	GC–FID	0.03–1.0	0.1–200	5–13	1–23	Wastewater	[52]
HSME[k]	GC–FID	4.0–41.0	10–480	0.7–19.5	–	Tap, pool, well, spring water, wastewater	[53]
μ-SPE[l]	HPLC–UV	0.026–0.82	0.2–100.0	3.8–9.8	75–114	Rain and river water	[54]
HS–SPME	GC–FID	0.02–0.09	0.5–100	3.2–7.8	81–112	Wastewater, well, tap water	[55]
SPE	HPLC–UV	0.01–0.06	0.1–300	3.2–11.4	64–119	Agricultural, tap water, wastewater	This work

[a] Liquid-phase microextraction.
[b] Gas chromatography-flame ionization detection.
[c] Low-density solvent demulsification dispersive liquid–liquid microextraction.
[d] Gas chromatography–mass spectrometry.
[e] Headspace solid-phase microextraction.
[f] Gas chromatography–isotope dilution mass spectrometry.
[g] Continuous-flow microextraction.
[h] Cloud point extraction.
[i] High-performance liquid chromatography-fluorescence.
[j] Microwave-assisted headspace solid-phase microextraction.
[k] Headspace solvent microextraction.
[l] Micro-solid-phase extraction.

This study was performed to achieve good recovery of PAHs from the SPE frit. In this experiment, different volumes of samples (50–1000 mL) were passed through the copolymer coated frit at 1 mL min^{-1} flow rate. The result shown in Fig. 8d indicates that different PAHs have different breakthrough volumes and therefore different preconcentration factors. Fig. 8d shows that increasing the sample volume (up to 500 mL) does not decrease the extraction efficiency of phenanthrene, anthracene, fluoranthene and pyrene but reduces the extraction efficiency of naphthalene, acenaphthylene, fluorene and biphenyle. Based on reproducible results (Fig. 8d), if a volume of 500 mL is used, the highest concentration factor is 5000 which belongs to phenanthrene, anthracene, fluoranthene and pyrene and, if a volume of 250 mL is used, the lowest concentration factor of 2500 is obtained for naphthalene, acenaphthylene, fluorene and biphenyle. To reach the high recovery rates and to reduce the time of analysis, loading volume was set to 50 mL in subsequent experiments.

3.4. Validation parameters

After optimizing various effective parameters, figures of merit including linear range (LR), precisions in terms of repeatability and reproducibility were evaluated by calculating the relative standard deviations (RSDs) and limit of detection (LOD) of the developed method (Table 1). The LR determined after extracting various aqueous solutions of the mixture of PAHs at eight concentration levels were between 0.1 and 300 ng mL^{-1}. The coefficients of determination (r^2) calculated for the calibration plots were between 0.9811 and 0.9973. The precision of the method reported in Table 1 was determined by seven replicate analyses from aqueous solutions containing 8 ng mL^{-1} of each PAH. As this table shows, the intra-day RSD% varied between 3.2% and 11.4%. The frit-to-frit precisions measured by three replicate analyses from aqueous solution containing 8 ng mL^{-1} of each PAH were between 2.4% and 10.3%. Table 1 also shows that the limits of detection, based on S/N=3, vary between 0.01 and 0.08 ng mL^{-1}.

In Table 2, a comparison is made between the figures of merit obtained in the present work and similar works reported by other research groups. The LODs and RSDs found in the present work are in some cases comparable or greater than the values reported for other coatings, despite the fact that some of them have used MS detection.

3.5. Real sample

Three different water samples including, tap water collected from the Shahid Bahonar University Campus (SBUC), wastewater collected from Zarand Coal Industry (Zarand, Iran), and agricultural

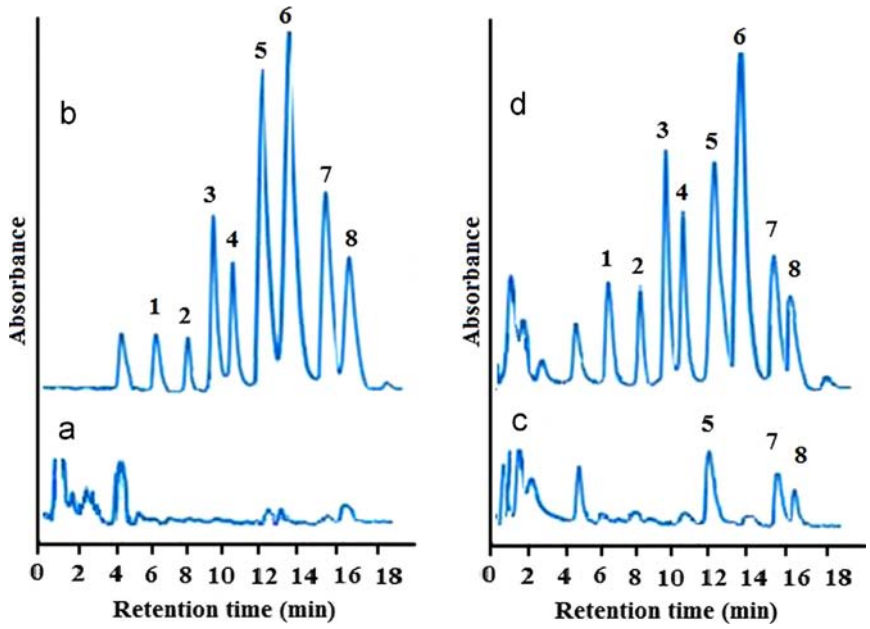

Fig. 9. HPLC–UV chromatograms of water samples: a) blank sample; b) standard sample; c) wastewater; d) tap water spiked with 40 ng mL^{-1} each PAH. Peaks: (1) Nap, (2) Acy, (3) Bip, (4), Flu (5) Phe, (6) Ant, (7) Flt, (8) Pyr.

Table 3
Results obtained for percent recovery.

Compound	Recovery (%)			
	Tap water		Wastewater	
	8 (ng mL^{-1})	40 (ng mL^{-1})	8 (ng mL^{-1})	40 (ng mL^{-1})
Nap	88	107	73	98
Acy	80	104	92	90
Bip	104	64	101	79
Flu	91	95	85	105
Phe	88	117	96	79
Ant	102	106	90	87
Flt	105	99	104	106
Pyr	104	119	89	91

water collected from near the coal industry were taken. Three replicate analyses were performed on each sample using the copolymer coated frit under optimal SPE conditions. Compound identification was confirmed using GC–MS. The results found for these analyses are shown in Table 1. None of the eight PAHs could be detected in tap water. A typical chromatogram is shown in Fig. 9. The analyte recovery of the method was evaluated by spiking two samples of SPE tap water and wastewater at 8 and 40 ng mL^{-1} of each PAH. The recoveries obtained were between 64% and 119% (Table 3).

4. Conclusion

Copolymerization of pyrrole and *o*-toluidine on a steel frit has resulted in a new SPE device. Chemical and mechanical resistance, reproducible synthesis, low cost and relatively long life span are the main advantages of this frit. It was the frit that provided a porous structure with high specific surface area and thus high extraction efficiency. In this study, the potential of a simple SPE device by using a copolymer coated frit, for the selective pre-concentration and determination of eight PAHs, has been explored. Using the designed device was simple for sample loading and eluting, and it needed no vacuum or pressure system. The method also showed satisfactory accuracy, linearity, detection limits and precision. It is worthy to note that due to high obtained extraction efficiencies for the analytes in the proposed method, by using sensitive detectors such as mass spectrometry or fluorescence, very small LODs can be obtained.

References

[1] E. Martinez, M. Gros, S. Lacorte, D. Barceló, J. Chromatogr. A 1047 (2004) 181–188.
[2] A. Nikolaou, M. Kostopoulou, G. Lofrano, S. Meric, A. Petsas, M. Vagi, Trends Anal. Chem. 28 (2009) 653–664.
[3] C. Anyakora, Handbook of Water Analysis, in: L.M.L. Nollet (Ed.), CRC Press, Boca Raton, FL, 2007, pp. 579–597.
[4] Y. Wan, X. Jin, J. Hu, F. Jin, Environ. Sci. Technol. 41 (2007) 3109–3114.
[5] J.P. Franke, R.A. de Zeeuw, J. Chromatogr. B 713 (1998) 51–59.
[6] Y.Y. Zhou, X.P. Yan, K.N. Kim, S.W. Wang, M.G. Liu, J. Chromatogr. A 1116 (2006) 172–178.
[7] H. Wu, X. Wang, B. Liu, J. Lu, B. Du, L. Zhang, J. Ji, Q. Yue, B. Han, J. Chromatogr. A 1217 (2010) 2911–2917.
[8] J. Jin, Z. Zhang, Y. Li, P. Qi, X. Lu, J. Wang, J. Chen, F. Su, Anal. Chim. Acta 678 (2010) 183–188.
[9] N. Pourreza, K. Ghanemi, J. Hazard. Mater. 161 (2009) 982–987.
[10] O. Wurl, in: O. Wurl (Ed.), Practical Guidelines for the Analysis of Seawater, CRC Press, Boca Raton, FL, 2009, pp. 329-349.
[11] K. Li, H. Li, L. Liu, Y. Hashi, T. Maeda, J.M. Lin, J. Chromatogr. A 1154 (2007) 74–80.
[12] J.N. Brown, B.M. Peake, Anal. Chim. Acta 486 (2003) 159–169.
[13] E. Lesellier, J. Chromatogr. A 1218 (2011) 251–257.
[14] P. Oleszczuk, S. Baran, J. Hazard. Mater. 113 (2004) 237–245.
[15] S. Zhang, H. Niu, Z. Hu, Y. Cai, Y. Shi, J. Chromatogr. A 1217 (2010) 4757–4764.
[16] W.D. Wang, Y.M. Huang, W.Q. Shu, J. Cao, J. Chromatogr. A 1173 (2007) 27–36.
[17] H. Bagheri, Z. Ayazi, A. Aghakhani, Anal. Chim. Acta 683 (2011) 212–220.
[18] Y.Y. Zhou, X.P. Yan, K.N. Kim, S.w. Wang, M.G. Liu, J. Chromatogr. A 1116 (2006) 172–178.
[19] S.H. Huo, X.P. Yan, Analyst 137 (2012) 3445–3451.
[20] J.H. Lin, Wei-Lung Tseng, Rev. Anal. Chem. 31 (2012) 153–162.
[21] B.A. Shah, C.B. Mistry, Sep. Sci. Technol. 48 (2013) 1717–1728.
[22] D.D. Borole, U.R. kapadi, P.P. Mahulikar, D.G. Hundivale, Mater. Lett. 58 (2004) 3816–3822.
[23] B.C. Roy, M.D. Gupta, J.K. Ray, Macromolecules 28 (1995) 1727–1732.
[24] X. Li, M. Huang, L. Wang, M. Zhu, A. Menner, J. Springer, Syn. Met. 123 (2001) 435–441.
[25] J.W. Kim, C.H. Cho, F. Liu, H.J. Choi, J. Joo, Syn. Met. 135–136 (2003) 17–18.
[26] S. Yalcinkaya, T. Tuken, B. Yazici, M. Erbil, Prog. Org. Coat. 63 (2008) 424–433.
[27] M.R. Mahmoudian, Y. Alias, W.J. Basirum, M. Ebadi, Curr. Appl. Phys. 11 (2011) 368–375.
[28] L.F. Warren, D.P. Anderson, J. Electrochem. Soc. 134 (1987) 101–105.

[29] W. Prissanaroon, N. Brack, P.J. Pigram, J. Liesegang, Sur. Rev. Lett 13 (2006) 319–327.
[30] A. Mollahosseini, E. Noroozian, Anal. Chim. Acta 638 (2009) 169–174.
[31] P. Olszowy, M. Szultka, P. Fuchs, R. Kegler, R. Mundkowski, W. Miekisch, J. Schubert, B. Buszewski, J. Pharm, Anal. 53 (2010) 1022–1027.
[32] J. Wu, Z. Mester, J. Pawliszyn, Anal. Chim. Acta 424 (2000) 211–222.
[33] J.C.C. Yu, E.P.C. Lai, Anal. Bioanal. Chem. 381 (2005) 948–952.
[34] H. Bagheri, M. Saraji, D. Barcelo, Chromatographia 59 (2004) 283–289.
[35] H. Bagheri, A. Mohammadi, A. Salemi, Anal. Chim. Acta 513 (2004) 445–449.
[36] F. Augusto, L.W. Hantao, N.G.S. Mogollon, S.C.G.N. Braga, Trends Anal. Chem. 43 (2013) 14–23.
[37] L. He, C.S. Toh, Anal. Chim. Acta 556 (2006) 1–15.
[38] A. Mehdinia, M.F. Mousavi, J. Sep. Sci. 31 (2008) 3565–3572.
[39] J. Wu, J. Pawliszyn, Anal. Chim. Acta 520 (2004) 257–264.
[40] G. Sabouraud, S. Sadki, N. Brodie, Chem. Soc. Rev. 29 (2000) 283–293.
[41] L. Bao, R. Xiong, W. Zhang, G. Wei, Chin. J. Chem. Phys. 24 (2011) 55–64.
[42] M.R. Mahmoudian, Y. Alias, W.J. Basirum, M. Ebadi, Curr. Appl. Phys. 11 (2011) 368–375.
[43] A.A. Boyd-Boland, J. Pawliszyn, J. Chromatogr. A 704 (1995) 163–172.
[44] L.H. Keith, W. Grummett, J. Deegan, R.A. Libby, J.K. Taylor, G. Wentler, Anal. Chem. 55 (1983) 2210–2218.
[45] A. Lagana, G. Goretti, B.M. Petronio, M. Rotatori, J. Chromatogr. A 219 (1981) 263–271.
[46] L.A. Berrueta., B. Gallo, F. Vicente, Chromatographia 40 (1995) 474–483.
[47] M.R.K. Zanjani, Y. Yamini, S. Shariati, J.Å. Jönsson, Anal. Chim. Acta 585 (2007) 286–293.
[48] L. Guo, H.K. Lee, J. Chromatogr. A 1218 (2011) 5040–5046.
[49] L. Campo, R. Mercadante, F. Rossella, S. Fustinoni, Anal. Chim. Acta 631 (2009) 196–205.
[50] Y. Liu, Y. Hashi, J.M. Lin, Anal. Chim. Acta 585 (2007) 294–299.
[51] B. Delgado, V. Pino, J.H. Ayala, V. González, A.M. Afonso, Anal. Chim. Acta 518 (2004) 165–172.
[52] M.C. Wei, J.F. Jen, Talanta 72 (2007) 1269–1274.
[53] S. Shariati-Feizabadi, Y. Yamini, N. Bahramifar, Anal. Chim. Acta 489 (2003) 21–31.
[54] Y. Huang, Q. Zhou, G. Xie, J. Hazard. Mater. 193 (2011) 82–89.
[55] M. Behzadi, E. Noroozian, M. Mirzaei, Talanta 108 (2013) 66–73.